

Recent Progress in Studies of Pulsar Wind Nebulae

Patrick Slane

Harvard-Smithsonian Center for Astrophysics

Abstract.

The synchrotron-emitting nebulae formed by energetic winds from young pulsars provide information on a wide range phenomena that contribute to their structure. High resolution X-ray observations reveal jets and toroidal structures in many systems, along with knot-like structures whose emission is observed to be time-variable. Large-scale filaments seen in optical and radio images mark instability regions where the expanding nebulae interact with the surrounding ejecta, and spectral studies reveal the presence of these ejecta in the form of thermal X-ray emission. Infrared studies probe the frequency region where evolutionary and magnetic field effects conspire to change the broadband synchrotron spectrum dramatically, and studies of the innermost regions of the nebulae provide constraints on the spectra of particles entering the nebula. At the highest energies, TeV gamma-ray observations provide a probe of the spectral region that, for low magnetic fields, corresponds to particles with energies just below the X-ray-emitting regime.

Here I summarize the structure of pulsar wind nebulae and review several new observations that have helped drive a recent resurgence in theoretical modeling of these systems.

Keywords: Pulsar Wind Nebulae; Pulsars; Supernova Remnants

PACS: 01.30.Cc;95.85.Hp;95.85.Nv;95.85.Pw;97.60.Gb;98.38.Mz

INTRODUCTION

It has long been known that the Crab Nebula is produced by the wind from a young, energetic pulsar whose spin-down power manifests itself as a synchrotron-emitting bubble of energetic particles. Optical observations reveal toroidal wisps and jet-like outflows near the pulsar. Faint portions of a ring are observed, marking the region where the pulsar wind undergoes a shock upon entering the surrounding nebula, the outer portions of which are rich in filamentary structure from swept-up ejecta. Though clearly formed in a supernova (SN) event in 1054 CE, the Crab shows no trace of an associated supernova remnant (SNR), presumably indicating that the SN blast wave is propagating through a very low density medium; the nebula results entirely from the pulsar input (and its confinement by surrounding material – in this case, stellar ejecta) and is the prototypical example of a pulsar wind nebula (PWN).

The diagram shown in Figure 1 illustrates the main points of the most basic picture for a PWN: in an inner zone the wind flows away from the neutron star (NS) with Lorentz factor $\gamma \sim 10^6$; at a distance R_w from the NS the wind passes through a termination shock, decelerating the flow while boosting particle energies by another factor of $\gtrsim 10^3$; and beyond R_w energetic electrons in the wind radiate synchrotron emission in the wound-up toroidal magnetic field to form the PWN which is confined at a radius R_{PWN} by the inertia of the SN ejecta or the pressure of the interior of a surrounding SNR. A

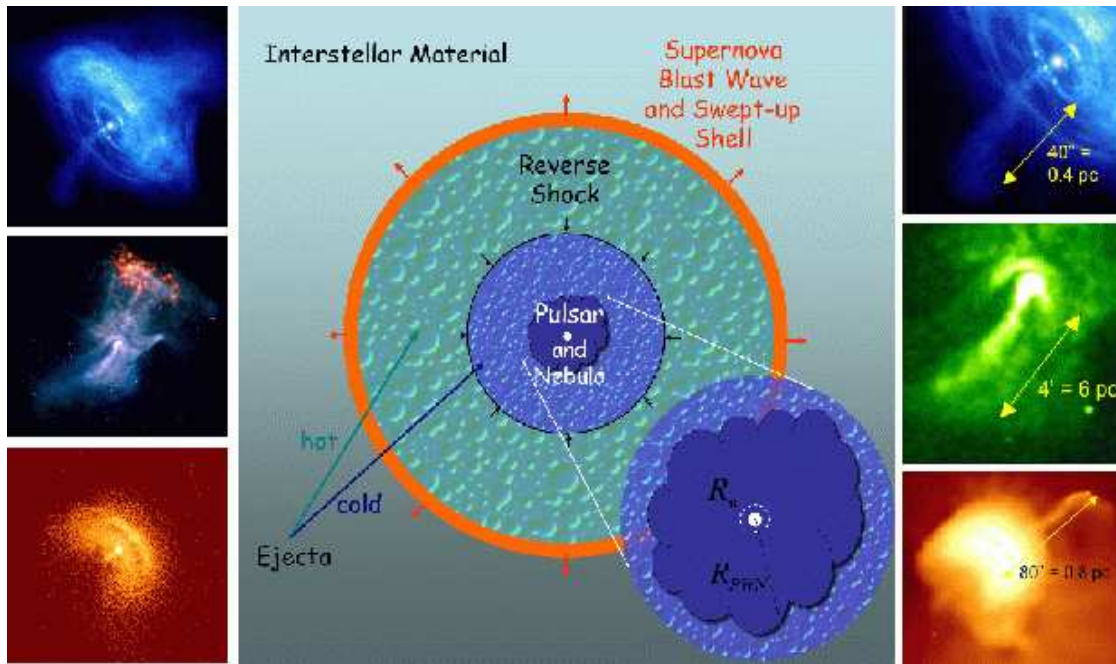


FIGURE 1. Schematic diagram of a PWN within an SNR (see text for description). *Chandra* images of the Crab Nebula, PSR B1509–58, and Vela are shown in the left panels. On the right are corresponding images of the jets in these nebula, with indications of the relative sizes. Here and throughout, north is up and east is to the left.

detailed theoretical framework, incorporating particle injection and diffusion, magnetic field evolution and radiative and adiabatic losses, has been constructed within this picture, allowing us to successfully predict and explain some basic PWN properties (Reynolds & Chevalier 1984; Kennel & Coroniti 1984). For a more detailed review on the structure and evolution of PWNe, see Gaensler & Slane (2006).

Most models of PWNe have been built and tailored to explain the properties of the Crab, but questions have lingered as to whether or not other PWNe were really well-described by this “prototype.” Recent observations, particularly with high resolution X-ray telescopes, have now shown that despite considerable differences in age, environmental conditions, and pulsar properties, a large number of PWNe share many of the Crab’s traits. In particular, it has become startlingly apparent that pulsars release their energy not in an isotropic fashion, but rather in equatorial winds and polar outflows defined by the spin axis of the system. In Figure 1 (left panels) we show *Chandra* images of the Crab Nebula (Weisskopf et al. 2000), PSR B1509–58 (Gaensler et al. 2002), and the inner nebula around the Vela pulsar (Helfand et al. 2001). Each shows a well-defined axis of symmetry associated with the spin axis of the pulsar, along with arc-like structures in the equatorial plane. Similar structures have now been identified around a large number of young pulsars. The symmetry extends to large scales as well, with enhanced confinement by the toroidal field producing nebulae whose extent along the spin axis is larger than at the equator (see Figure 2). In the extended nebulae, particles suffer synchrotron losses which gradually steepen the spectra with radius, as the higher energy

particles are burned off as they diffuse toward the outer boundary – an effect readily observed in X-ray spectra of PWNe (e.g. Slane et al. 2001, Slane et al. 2004) that directly probes the efficiency of the synchrotron cooling (Chevalier 2000).

JET/TORUS STRUCTURE IN PWNE

As indicated above, when the free-flowing equatorial wind from the pulsar encounters the more slowly-expanding nebula, a termination shock is formed at the radius, R_w , at which the ram pressure of the wind is balanced by the internal pressure of the PWN:

$$R_w = \sqrt{\dot{E} / (4\pi\omega c \mathcal{P}_{\text{PWN}})}, \quad (1)$$

where ω is the equivalent filling factor for an isotropic wind, and \mathcal{P}_{PWN} is the total pressure in the shocked nebular interior. Upstream of the termination shock, the particles do not radiate, but flow relativistically along with the frozen-in magnetic field. At the shock, particles are thermalized and re-accelerated, forming a toroidal emission region in the downstream flow. Emission from the termination shock region and the downstream torus is seen clearly in the Crab Nebula (see upper left in Figure 1); the geometry implied by the X-ray morphology is a tilted torus, with a jet of material that flows along the toroid axis, extending nearly 0.4 pc from the pulsar (see upper right in Figure 1). A faint counter-jet accompanies the structure, and the X-ray emission is significantly enhanced along one edge of the torus. Both effects are presumably the result of Doppler beaming of the outflowing material, whereby the X-ray intensity varies with viewing angle. Estimates of the nebular pressure are in good agreement with the observed termination shock position based on the measured \dot{E} (see Eq. 1).

Similar geometric structures have now been observed in a number of PWNe. *Chandra* observations of G54.1+0.3 (Figure 3), for example, reveal a central point-like source surrounded by an X-ray ring whose geometry suggests an inclination angle of about 45° (Lu et al. 2002). The X-ray emission is brightest along the eastern limb of the ring. If interpreted as the result of Doppler boosting, this implies a post-shock flow velocity of $\sim 0.4c$. The ring is accompanied by faint bipolar elongations aligned with the projected axis of the ring, consistent with the notion that these are jets along the pulsar rotation axis.

The formation of these jet/torus structures can be understood as follows (see Lyubarsky 2002). Outside the pulsar magnetosphere, the particle flow is radial. The rotation of the pulsar forms an expanding toroidal magnetic field for which the Poynting flux decreases with increasing latitude. Conservation of energy flux along flow lines thus results in a variation of the wind magnetization parameter, σ (the ratio of Poynting flux energy density to that in particles), and this anisotropy results in the toroidal structure of the downstream wind. Modeling of the flow conditions across the shock shows that magnetic collimation produces jet-like flows along the rotation axis (Komissarov & Lyubarsky 2004). This collimation is highly dependent on the magnetization of the wind. At high latitudes σ is large, resulting in a small termination shock radius and strong collimation, while close to the equator σ is much smaller and the termination shock extends to larger radii.



FIGURE 2. *Chandra* image of 3C 58, from co-added images in the 0.5-1.0 keV (red), 1.0-1.5 keV (green), and 1.5-10 keV (blue) bands. The PWN is elongated in the E-W direction, along spin axis defined by the jet direction. A shell of soft (red) thermal emission is evident, as is a complex of synchrotron loops and filaments.

The jets observed in PWNe differ considerably from source to source, spanning a large range in size (see right panels in Figure 1) and in luminosity (relative to both that of the nebula and to the available spin-down power of the pulsar). At present, the connection between the observed structure and the properties of the pulsar and its environment is not well understood. The jets shown in Figure 1 all exhibit some amount of curvature, and this is typical of most pulsar jets (e.g., that in 3C 58 – see Figure 4). The hoop stresses thought to confine the jets are subject to kink instabilities, which can result in deflections of the flow, possibly explaining the observed structures. The morphology of the Vela pulsar jet, shown in Figure 1, is observed to change rapidly with time, consistent with the presence of such instabilities.

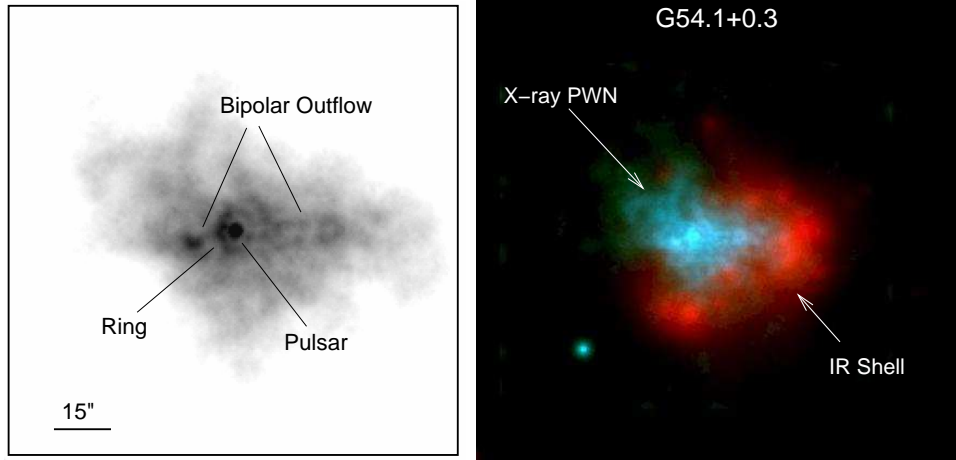


FIGURE 3. Left: *Chandra* image of G54.1+0.3 revealing a ring-like structure surrounding the pulsar as well as jet-like outflows extending into a diffuse nebula. Right: Composite showing *Chandra* image (blue) and *Spitzer* image (MIPS 24 μm). The IR observations reveal a shell in which the PWN is embedded.

PWN ENVIRONMENTS

While the SNR shell for the Crab Nebula has yet to be identified, there is ample evidence for ejecta from its progenitor in the form of Rayleigh-Taylor filaments formed as the relativistic gas in the nebula expands into the slower-moving, denser ejecta. These are clearly seen in optical and infrared line maps of the Crab, and also in radio observations where the synchrotron emission is enhanced along the filaments due to compression of the magnetic field. There appears to be little dust in the Crab's environment, however; *Spitzer* observations indicate a total dust mass of $< 1 M_{\odot}$, with virtually no emission from small grains (Temim et al. 2006). Searches for an SNR shell continue, for the Crab and other young PWNe, because of the considerable information such a detection would provide, in particular on the composition and density profile of the ejecta through which the young nebulae are expanding.

Optical studies of 3C 58 reveal filamentary structures associated with ejecta (van den Bergh 1978; Rudie & Fesen 2007), and X-ray observations reveal a shell of shock-heated material with enhanced abundances, suggesting an ejecta origin (Bocchino et al. 2001, Slane et al. 2004, Gotthelf et al. 2006). This is illustrated in Figure 2 where we show a *Chandra* image that reveals extended low energy emission enriched in Ne (shown in red) in the outer regions of the PWN. The total mass of this material, along with the size of the nebula, suggest an age of several thousand years (Chevalier 2005), calling into question the often-assumed historical association of 3C 58 with SN 1181.

In addition to the soft X-ray shell, the *Chandra* observations of 3C 58 reveal a network of synchrotron loops and filaments spread throughout the nebula whose nature is currently unknown. Unlike the radio filaments seen in the Crab, these structures do not seem to correspond well with the optical filaments in 3C 58. Kink instabilities can lead to loops of magnetic flux being torn from the pulsar jet regions, and these could manifest themselves as regions of enhanced synchrotron emission, but more studies are required to determine whether these structures are unique to 3C 58.

The outer regions of the diffuse X-ray emission in G54.1+0.3 show a softer spectrum than the interior regions, but there is no evidence for a thermal X-ray component associated with shock-heated ejecta or ISM. *IRAS* observations reveal excess infrared emission above the extrapolated synchrotron spectrum, however. Recent *Spitzer* observations (Slane et al., in preparation) reveal a shell of emission that may be associated with the swept-up ejecta or shocked dust (Figure 3, right). Of particular interest is a complex of infrared knots in the western portion of the shell, directly in line with the termination of the jet-like outflow seen in X-rays (Figure 3, left). Further IR spectroscopy is required to determine the nature of the shell and its association with G54.1+0.3.

BROADBAND SPECTRA OF PWNE

The broadband spectrum of a pulsar wind nebula (PWN) is determined by the input spectrum from the pulsar, as modified at the termination shock where the pulsar wind joins the flow in the nebula, incorporating the evolution of the nebula magnetic field strength as the nebula expands into the ambient medium. For a power-law injection of particles from the pulsar, a constant magnetic field in the nebula yields a power law

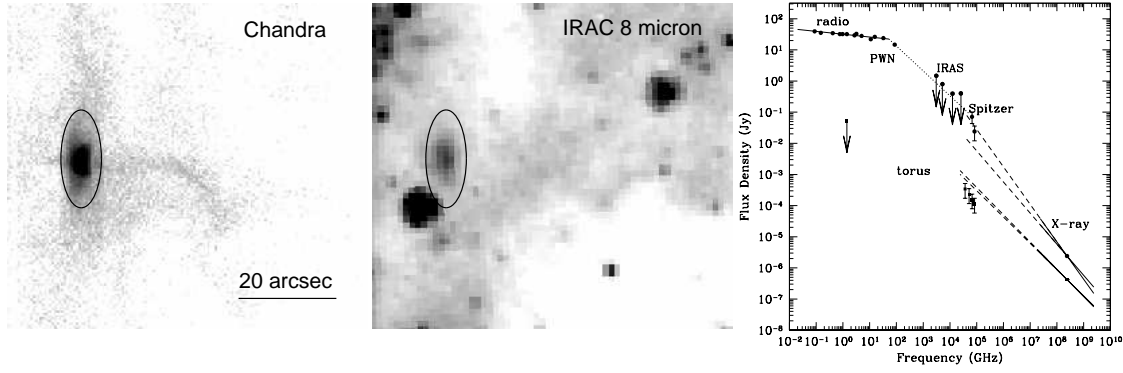


FIGURE 4. Left: *Chandra* image of the pulsar, torus, and jet in 3C 58. Center: *Spitzer* image (IRAC 8 μm) revealing the 3C 58 torus. Right: Broadband spectrum for 3C 58 and its torus, indicating that a broken spectrum is injected into the nebula from the termination shock region.

synchrotron spectrum with a break at a frequency

$$\nu_b \approx 10^{21} B_{\mu\text{G}}^{-3} t_3^{-2} \text{ Hz} \quad (2)$$

(where $B_{\mu\text{G}}$ is the magnetic field strength, in μG , and t_3 is the age in units of 10^3 yr) above which the synchrotron cooling time of the radiating particles is less than the age of the nebula. Additional contributions to the spectral structure in PWNe include the effects of any time-dependent input from the pulsar, of the interaction of SNR reverse shock with the PWN, and of any features in the injection spectrum itself.

Typically, PWN spectra are characterized by a flat power law index at radio frequencies ($\alpha \approx -0.3$, where $S_\nu \propto \nu^\alpha$) and a considerably steeper index in X-rays ($\alpha \sim -1$). The Crab Nebula has a spectral break at $\sim 10^{13}$ Hz, interpreted as a cooling break from a $\sim 300\mu\text{G}$ field, as well as breaks at $\sim 3 \times 10^{14}$ Hz and ~ 40 keV. There is a class of PWNe with breaks at much lower frequencies, however; 3C 58, for example, has a break at ~ 50 GHz which, if interpreted as a cooling break would imply a magnetic field well in excess of 1 mG – an unreasonably high field for a PWN, and one inconsistent with the fact that the X-ray emission from 3C 58 extends all the way to the radio edge of the nebula, indicating that no synchrotron loss breaks occur far below the X-ray band.

Spitzer observations of 3C 58 (Slane et al. - in preparation) show that the mid-IR emission from this PWN is consistent with extrapolation of the X-ray spectrum. Of particular interest, though, is that that pulsar torus is also detected in *Spitzer* observations (Figure 4). The resulting spectrum requires at least one spectral break, implying that the particle spectrum injected into the nebula is not a single power law. Further characterization of the emission in this region is of considerable importance for proper modeling of the evolved nebular spectrum.

HIGH ENERGY EMISSION FROM PWNE

Recent discoveries of very high energy γ -ray emission associated with PWNe have opened a new channel for investigations of the structure and evolution of these objects.

Of particular interest is Vela X, the large wind nebula associated with the Vela pulsar. It is located to the south of the pulsar, but this offset position cannot be attributed to the pulsar velocity because the direction of the pulsar motion, known from radio VLBI observations, is not directed away from the center of the nebula. Blondin et al. (2001) explained Vela X as a PWN that has been crushed and pushed off-center by an asymmetric reverse shock wave that resulted from the supernova interaction with an asymmetric surrounding medium. *ROSAT* observations of the Vela SNR revealed a hard emission component extending southward from the pulsar, into the Vela X region (Markwardt & Ögelman 1995) and a filamentary radio structure extends alongside the same region. HESS observations reveal an extended region of TeV emission that follows this same structure (Aharonian et al. 2006), presumably tracing filamentary structure produced by the interaction of the PWN with the reverse shock.

This emission in the TeV band probably originates from inverse-Compton scattering of ambient soft photons with energetic electrons in the nebula (Aharonian et al. 2006), although models have been considered in which the emission is associated with the decay of neutral pions produced in collisions of energetic ions with ambient hadronic material (Horns et al. 2006). If correct, the latter interpretation would be of particular importance because it would demonstrate the presence of ions in the pulsar wind. Enhanced pion production from such a wind may result from the mixing of ejecta material into the PWN through instabilities produced by the reverse shock interaction. Indeed, X-ray observations indicate the presence of shocked ejecta material within the Vela X region (LaMassa, Slane, & de Jager, in preparation), strengthening the case for the reverse-shock interaction scenario and potentially providing hadronic material with which an ionic wind might interact to produce pions. However, further observations of the high energy spectrum are required to differentiate between the two emission scenarios.

Several recently-discovered HESS sources in the Galactic plane also seem likely to be associated with PWNe. They are extended, have spectra consistent with other PWNe, and have young radio pulsars nearby. Examples include HESS J1804-216, HESS J1825-137, and HESS J1718-385 (Aharonian et al. 2005, Aharonian et al. 2007). For each of these sources, the young pulsars suggested as the engines for these nebulae are distinctly separated from the TeV centroids, possibly suggesting that the PWNe have been disturbed by an asymmetric reverse shock interaction as proposed for Vela X. In most cases, however, the surrounding SNRs have yet to be identified.

In addition to the nature of the curious morphology for these sources, a more vexing question centers on their very large sizes. Several of these sources are observed to be extended on scales as large as 15-30 arcmin or more. Using the dispersion-measure distances of the pulsars which are suspected to have created the nebulae, the physical sizes are in excess of 15 pc – much larger than any known PWNe observed in the radio or X-ray bands. Diffusion of low energy particles to distances far from the pulsar has been suggested as an explanation for this large size. However, detailed modeling of the environment that would lead to such a nebula, in the context of the reverse shock interaction scenario, has yet to be carried out. The results from these and other TeV observations are thus driving new investigations of PWN structure and evolution.

SUMMARY

Recent advances in observations of PWNe have uncovered a wealth of information regarding the axisymmetric nature of the wind and the large- and small-scale structure of the nebulae. It is now clear that the Crab Nebula is indeed the prototypical member of this class – albeit a particularly bright and energetic example; the elongated nebula, swept-up ejecta, toroidal structure, and jets that characterize the Crab are now being found in a multitude of PWNe. Observations across the electromagnetic spectrum are helping to characterize the evolution of PWNe, and opening new questions regarding the nature of the wind and its interactions with its environs. These, in turn, have stimulated new theoretical work on relativistic flows, shocks, and jets with application to a broad range of topics in high energy astrophysics.

ACKNOWLEDGMENTS

I would like to thank the conference organizers for the opportunity to present this work, and also Bryan Gaensler, Jack Hughes, David Helfand, Steve Reynolds, and my many other colleagues with whom I have worked on studies of pulsar winds.

REFERENCES

1. F. Aharonian, et al., *Science* **307**, 1938 (2005).
2. F. Aharonian, et al., *A&A* **448**, L43 (2006).
3. F. Aharonian, et al., *A&A* **472**, 489 (2007).
4. J. M. Blondin, R. A. Chevalier, and D. M. Frierson, *ApJ* **563**, 806 (2001).
5. F. Bocchino et al., *A&A* **369**, 1078 (2001).
6. R. A. Chevalier, *MmSAI* **69**, 977 (1998).
7. R. A. Chevalier, *ApJ* **619**, 839 (2005).
8. B. M. Gaensler et al., *ApJ* **569**, 878 (2002).
9. B. M. Gaensler and P. O. Slane, *ARA&A* **44**, 17 (2006).
10. E. V. Gotthelf et al., *ApJ* **654**, 267 (2007).
11. D. J. Helfand et al., *ApJ* **556**, 380 (2001).
12. D. Horns et al., *A&A* **451**, L51 (2006).
13. C. F. Kennel and F. V. Coroniti, *ApJ* **283**, 694 (1984).
14. S. Komissarov and Y. E. Lyubarsky, *Ap&SS* **293**, 107 (2004).
15. F. J. Lu et al., *ApJ* **568**, L49 (2002).
16. Y. E. Lyubarsky, *MNRAS* **329**, L34 (2002).
17. C. Markwardt and H. Ögelman, *Nature* **375**, 40 (1995).
18. S. P. Reynolds, and R. A. Chevalier, *ApJ* **278**, 630 (1984).
19. G. C. Rudie and R. A. Fesen, *RMxAC* **30**, 90 (2007).
20. P. Slane et al., *ApJ* **533**, L29 (2000).
21. P. Slane et al., *ApJ* **616**, 403 (2004).
22. T. Temim et al., *ApJ* **132**, 1610 (2006).
23. S. van den Bergh, *ApJ* **220**, L9 (1978).
24. M. C. Weisskopf et al., *ApJ* **536**, L81 (2000).